coatings

MDPI

Article

Corrosion Resistance and Durability of Superhydrophobic Copper Surface in Corrosive NaCl Aqueous Solution

Chun-Wei Yao [1,*], Divine Sebastian [1], Ian Lian [2], Özge Günaydın-Şen [3], Robbie Clarke [1], Kirby Clayton [1], Chiou-Yun Chen [1], Krishna Kharel [3], Yanyu Chen [4] and Qibo Li [4]

1 Department of Mechanical Engineering, Lamar University, Beaumont, TX 77710, USA; dsebastian1@lamar.edu (D.S.); rclarke@lamar.edu (R.C.); kirbyelizabethclayton@gmail.com (K.C.); cchen4@lamar.edu (C.-Y.C.)
2 Department of Biology, Lamar University, Beaumont, TX 77710, USA; ilian@lamar.edu
3 Department of Chemistry and Biochemistry, Lamar University, Beaumont, TX 77710, USA; osen@lamar.edu (Ö.G.-Ş.); kkharel@lamar.edu (K.K.)
4 Transportation and Hydrogen Systems Center, National Renewable Energy Laboratory, Golden, CO 80401, USA; yanyu.chen@alumni.stonybrook.edu (Y.C.); li3902@tamu.edu (Q.L.)
* Correspondence: cyao@lamar.edu; Tel.: +1-409-880-7008

Received: 20 December 2017; Accepted: 9 February 2018; Published: 11 February 2018

Abstract: Artificial superhydrophobic copper surfaces play an important role in modern applications such as self-cleaning and dropwise condensation; however, corrosion resistance and durability often present as major concerns in such applications. In this study, the anti-corrosion properties and mechanical durability of superhydrophobic copper surface have been investigated. The superhydrophobic copper surfaces were achieved with wet chemical etching and an immersion method to reduce the complexity of the fabrication process. The surface structures and materials were characterized using scanning electron microscope (SEM), energy dispersive X-ray spectroscopy (EDX), and Fourier transform infrared spectrometer (FTIR). The corrosion resistance and mechanical properties of the superhydrophobic copper surface were characterized after immersing surfaces in a 3.5 wt % NaCl solution. The chemical stability of the superhydrophobic copper surface in the NaCl solution for a short period of time was also evaluated. An abrasion test and an ultrasound oscillation were conducted to confirm that the copper surface contained durable superhydrophobic properties. In addition, an atomic force microscope was employed to study the surface mechanical property in the corrosion conditions. The present study shows that the resulting superhydrophobic copper surface exhibit enhanced corrosion resistance and durability.

Keywords: superhydrophobic copper surface; anti-corrosion; durability; AFM

1. Introduction

Every natural phenomenon bears special features and properties. For instance, a feature of the lotus leaf is the behavior by virtue of which its surface repels water. The action in which a surface repels water droplets is called hydrophobic behavior and has vast implication in engineering applications. A hydrophobic surface requires a suitable type of morphology, specifically roughness, on the right materials exhibiting low surface free energy [1–4]. Scientists currently employ various methods for the fabrication and study of superhydrophobic surfaces, including chemical etching [5], chemical vapor deposition [6], solution immersion method [7], sol-gel method [8], and laser fabrication [9].

Notably, superhydrophobic surfaces that possess apparent contact angles greater than 150° have been investigated for applications in areas of self-cleaning [10], anti-icing [11], electronic cooling [12,13],

and dropwise condensation [14]. In such applications, copper, which has excellent conductive properties, is widely used as substrate material and turned into superhydrophobic surfaces. However, previous literature has primarily focused on thermal performance, such as heat transfer rate, in applications. To date, few methods have been presented for the fabrication of superhydrophobic copper surfaces for corrosion protection [15–18]. Durability and corrosion resistance of a superhydrophobic copper surface are still questions in implementation.

The main goal of the present study is to investigate the corrosion resistance and durability of superhydrophobic copper surfaces. In this research, superhydrophobic copper surfaces were fabricated by taking advantage of the nanostructures and the alteration of surface chemistry. The chemical stability of the superhydrophobic copper surfaces in the corrosive NaCl aqueous solution (3.5 wt %) for a short period of time were evaluated. The corrosion resistances were characterized by electrochemical methods after immersing surfaces in the NaCl solution. To test the durability of the superhydrophobic copper surfaces, mild abrasion testing and ultrasound oscillation were conducted. In addition, the degradation of the mechanical property after immersing the superhydrophobic copper surfaces in the NaCl solution was also investigated by using an atomic force microscope (AFM). The results of the morphology, mechanical property and non-wetting performance of the superhydrophobic copper surface exposed to corrosive medium highlighted the superior anti-corrosive properties of the surface.

2. Materials and Methods

C101 copper plates were used as test samples throughout the experiments performed. Sodium chlorite ($NaClO_2$) (Cole-Parmer, Vernon Hills, IL, USA), sodium hydroxide pellets (NaOH) (Cole-Parmer, Vernon Hills, IL, USA), and sodium phosphate tribasic dodecahydrate ($Na_3PO_4{\cdot}12H_2O$) (Sigma-Aldrich, St. Louis, MO, USA) were used along with deionized water to prepare an alkaline solution. Trichloro(1H,1H,2H,2H-perfluorooctyl) silane (Sigma-Aldrich, St. Louis, MO, USA) was used for the functionalization of the hierarchical copper oxide structure. Toluene (Sigma-Aldrich, St. Louis, MO, USA) was used as a solvent to dilute the solution of Trichloro(1H,1H,2H,2H-perfluorooctyl) silane. Experiments were conducted at room temperature of 23 °C.

The flat copper substrates, dimensions 5 cm by 5 cm by 0.5 mm, were initially cleaned using ultrasonication in acetone followed by rinsing with isopropyl alcohol, ethanol, and deionized water to clean off surface contaminants and grease. After the initial cleaning, the substrates were immersed in 2 M HCl to etch away the native oxide film present on the surfaces and named as pristine copper surface. The obtained pristine copper surfaces were then immersed in a hot alkaline solution composed of $NaClO_2$, NaOH, $Na_3PO_4{\cdot}12H_2O$ and deionized water in a weight proportion of 3.5:5:10:100 [19–21] maintained at 93 °C for a duration of 10 min. During this hot immersion, it was observed that the color of copper substrates gradually darkened to form a greyish texture on the surfaces. The substrates were then functionalized using Trichloro(1H,1H,2H,2H-perfluorooctyl) silane in Toluene solution with 1 mM concentration for a duration of 25 min [22]. After the functionalization process, the processed substrates were oven dried at 70 °C for 1 h and designated as a superhydrophobic copper surface. For preparing pristine copper substrates coated with Trichlorosilane, designated the reference surface, the processes remained the same except for immersing the substrates in the alkaline solution.

The morphologies and chemical compositions of the superhydrophobic copper surfaces were assessed using a scanning electron microscope (SEM, Hitachi S-3400N, Hitachi High Technologies, Tokyo, Japan) equipped with energy-dispersive X-ray spectroscopy, an atomic force microscope (AFM, Park NX10, Park System Co., Suwon, Korea), and a Fourier-transform infrared spectrometer (Nicolet iS50 FT-IR Spectrometer, Thermo Fisher Scientific, Waltham, MA, USA). The water contact angles were measured using a contact angle goniometer (ramé-hart instruments co., Succasunna, NJ, USA). Water droplets (5 μL) were carefully dropped onto the copper surfaces under ambient temperature and atmosphere. Electrochemical measurements were performed in a 3.5 wt % aqueous solution of NaCl at room temperature using a potentiostat system (Autolab PGSTAT204, Metrohm, Riverview, FL, USA). A stainless steel electrode, the superhydrophobic copper surface, and a silver/silver chloride (Ag/AgCl)

reference electrode were used as the counter electrode, working electrode, and reference electrode, respectively. The exposed area of the working electrode was 16.9 cm^2 for the calculation of corrosion rate. The current density was based primarily on the exposed geometrical area. The potentiodynamic anodic polarization curves were recorded at a sweep rate of 1 mV/s from −250 to 250 mV versus the open circuit potential.

3. Results and Discussion

3.1. Surface Morphologies and Chemical Compositions

Figure 1 shows the SEM image of the superhydrophobic copper surfaces and pristine copper surfaces. Micro-scratches/grooves can be seen on the pristine copper surfaces. At nano-scale, the superhydrophobic copper surfaces appear as leaf-like structures. These sharp and dense structures contribute to the high roughness associated with the substrates after processing. The energy-dispersive X-ray spectroscope (EDX) was used to verify the chemical composition of the surface, as Figure 2 shows. EDX data indicated that the surface includes Cu and O, suggesting CuO leaf-like nanostructures on the surface. Figure 3 shows the three-dimensional AFM image of the superhydrophobic copper surface. The average surface roughness of the surfaces was found to be 428 ± 12 nm, a relatively high number in terms of meeting the roughness requirements for a highly water repellent nature. The FTIR spectrum was recorded in the range from 400 to 4000 cm^{-1} with 320 scans and 2 cm^{-1} resolution to characterize chemical nature of the superhydrophobic surface. The few micrometers-thick top layer on the fabricated superhydrophobic surface was scraped off using a razor blade. The sample in powdered form was mixed with KCl to form isotropic pellets with 1% loading in mid IR region. Figure 4 shows the FTIR spectrum obtained for the superhydrophobic copper surface. A broad peak around 3411 cm^{-1} along with the peak around 1606 cm^{-1} accounts for OH stretching vibration [23–26]. A sharp peak at 614 cm^{-1} is accounted by the presence of halogens such as chlorine and fluorine [23,26]. The Si-O-Si stretching is evident at 1091 cm^{-1} [23,25], whereas Si–O rocking is characterized around 419 cm^{-1} [27]. Overlapping of PO_4^{3-} with SiO_4^{4-} can be observed at 504 cm^{-1} [28]. The weak band around 953 cm^{-1} is due to the presence of Si–O–Cu vibration [25] which suggests that the coating film is covalently attached to the copper substrate. The bands at wavenumbers 419 cm^{-1}, 504 cm^{-1}, 953 cm^{-1} and 1091 cm^{-1} indicate the covalent bond between silicon and oxygen that may have formed during the functionalization process. The small peak near 1317 cm^{-1} is assigned to the CF_2 functional group [29,30]. The peak around 1395 cm^{-1} is due to the presence of the aryl group. The presence of the C–H bond accounts for the peak at 2921 cm^{-1} [24,31]. In terms of the water contact angle, the measured average angle was 83° for pristine copper surface, 110° for the copper surface coated with Trichlorosilane (reference surface), and 169° for the superhydrophobic copper surface.

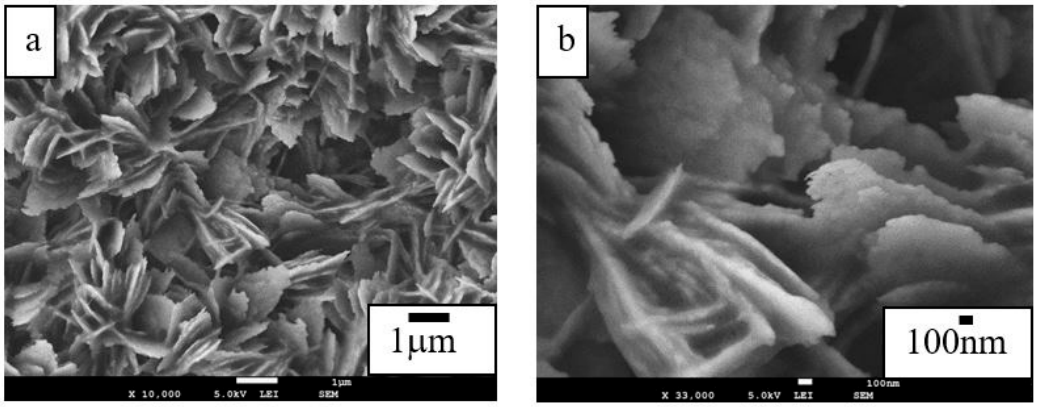

Figure 1. *Cont.*

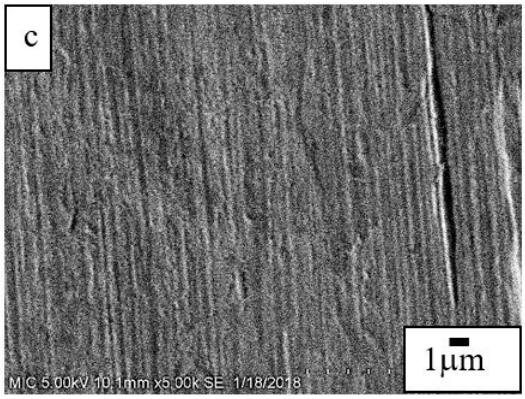

Figure 1. SEM images: (**a**) the superhydrophobic copper surface; (**b**) the superhydrophobic copper surface at higher magnification; (**c**) the pristine copper surface.

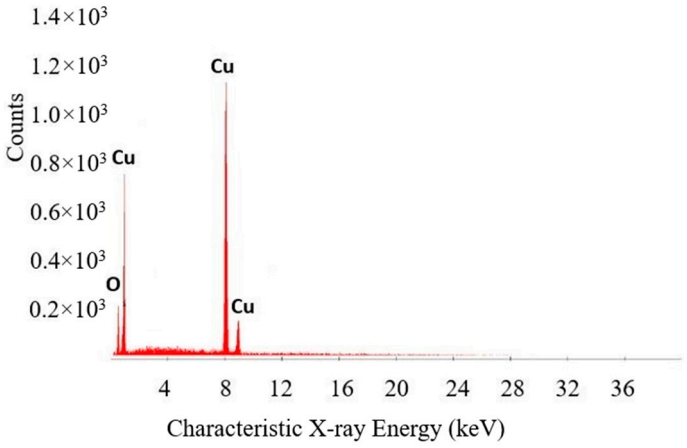

Figure 2. EDX spectrum analysis of the superhydrophobic copper surface.

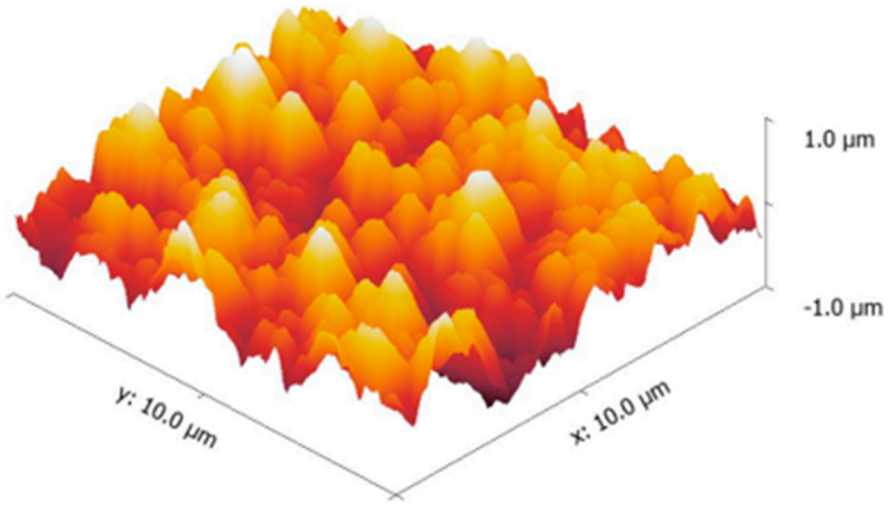

Figure 3. 3-Dimensional AFM image of the superhydrophobic copper surface.

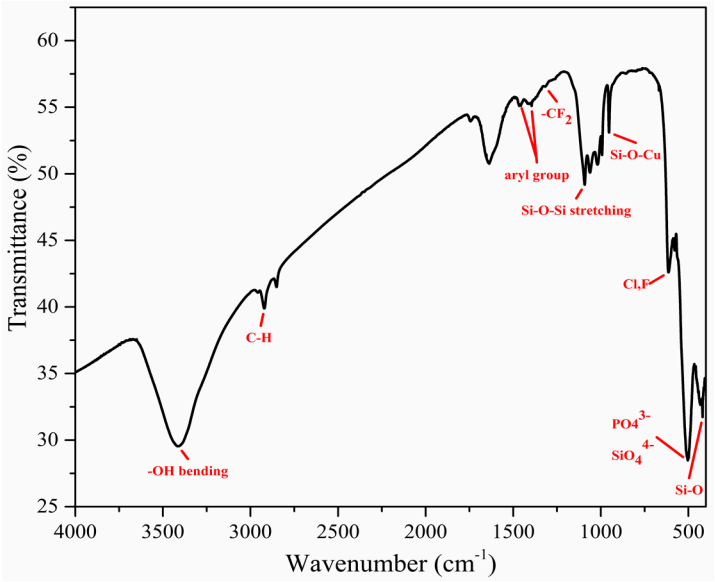

Figure 4. FTIR spectrum of the superhydrophobic copper surface.

3.2. Chemical Stability and Corrosion Resistance

Figure 5 shows the variation in the water contact angles of the superhydrophobic copper surfaces that were immersed in the 3.5 wt % NaCl aqueous solution. The static contact angles did not deviate considerably with respect to an increase in immersion time. Even after 24 h of immersion time, the static contact angle remained around 169°, which indicates that the surfaces maintain superhydrophobicity.

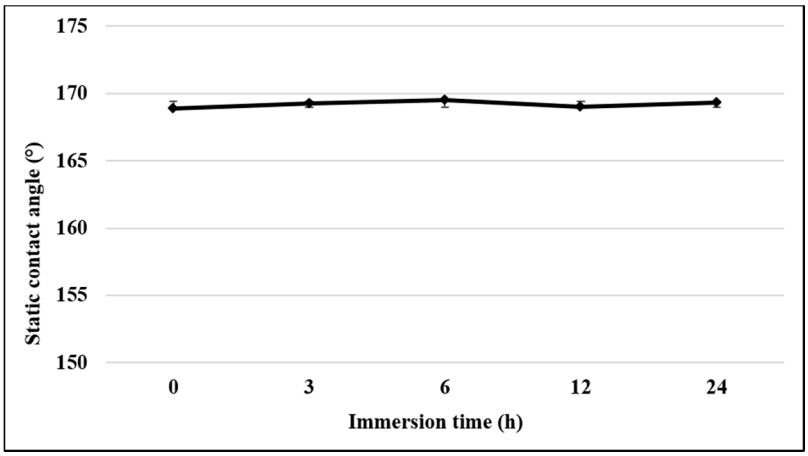

Figure 5. Effect of immersion time on the static water contact angle of the superhydrophobic copper surface.

Corrosion rate analysis was performed on the superhydrophobic copper surface using the potentiodynamic polarization method. All samples were immersed in a 3.5 wt % NaCl solution for one hour before each measurement was taken. The potentiodynamic polarization curve of the superhydrophobic copper surface was compared to the curves of pristine copper surface and copper surface coated with Trichlorosilane (reference surface), as shown in the Figure 6. Table 1 summarizes the corrosion potential (E_{corr}) and corrosion current density (j_{corr}). The corrosion potential for the pristine copper surface was less than −219 mV; whereas, the corrosion potential for the superhydrophobic

copper surface exceeded 105 mV. Moreover, the corrosion current density of the superhydrophobic surface was less than 1% that of the pristine copper surface. The corrosion rate can be calculated from

$$R = EW \times J \times K/\rho \quad (1)$$

where R is the corrosion rate (mm/year), EW is the equivalent weight of metal, J represents corrosion current density, K is a constant equal to 3272 [mm/(A·cm·year)]. ρ represents the density of the metal [32]. The exposed geometrical area of the surfaces was used to calculate the current density. The superhydrophobic surface exhibited a very low corrosion rate, which is a reduction of two orders of magnitude from that of the pristine copper surface or the copper surface coated with Trichlorosilane (reference surface), as shown in Table 1. This high-degree reduction in corrosion behavior can be accounted for by the interaction between the electrolyte solution and the surface, due to its liquid-repelling behavior. According to the Cassie-Baxter model, since air can be trapped within the leaf-like nanostructures, the liquid solution has difficulty penetrating the surface structures. Therefore, the trapped air can also inhibit a corrosive solution's ability to penetrate into surface structures [33]. Based on all the results discussed above, it can be concluded that the effect of the trapped air in the nanostructures is more significant than the effect of the silane layer in accounting for the superior corrosion resistance. Therefore the superhydrophobic copper surface possesses favorable corrosion resistance for the Cu substrate.

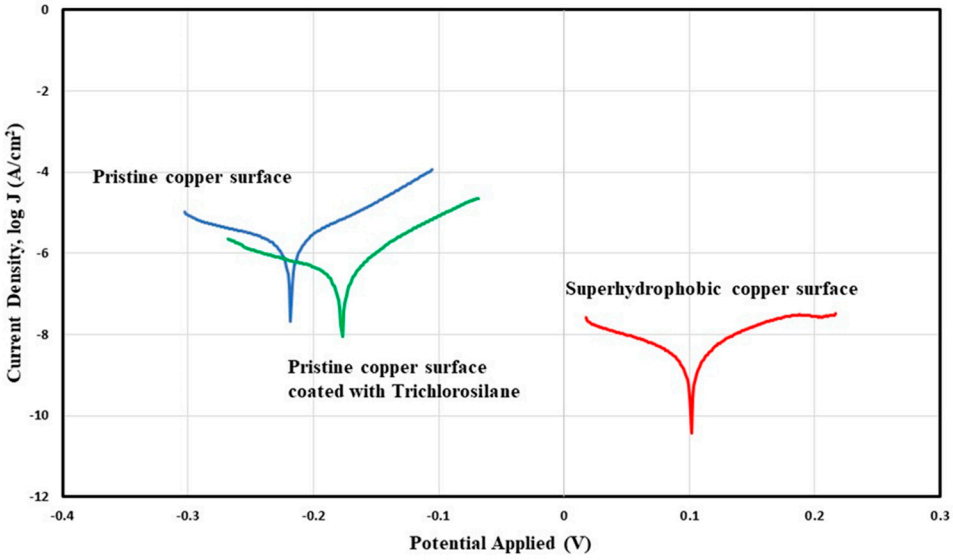

Figure 6. Potentiodynamic polarization curve obtained by using Ag/AgCl electrode as the reference electrode and 3.5 wt % NaCl solution as the electrolyte for pristine copper surface, copper surface coated with Trichlorosilane (reference surface), and superhydrophobic copper surface.

Table 1. Corrosion Potential (E_{corr}), Corrosion Current Density (J_{corr}), and Corrosion Rate of the pristine copper surface, copper surface coated with Trichlorosilane (reference surface), and superhydrophobic copper surface.

Sample	E_{corr} (V)	J_{corr} (A/cm^2)	Corrosion Rate (mm/year)
Pristine copper surface	$-2.20 \times 10^{-1} \pm 1.00 \times 10^{-3}$	$2.12 \times 10^{-6} \pm 4.02 \times 10^{-7}$	$4.89 \times 10^{-2} \pm 9.63 \times 10^{-3}$
Copper surface coated with Trichlorosilane	$-1.7 \times 10^{-1} \pm 8.91 \times 10^{-3}$	$6.6 \times 10^{-7} \pm 5.83 \times 10^{-7}$	$1.53 \times 10^{-2} \pm 1.35 \times 10^{-2}$
Superhydrophobic copper	$10.6 \times 10^{-2} \pm 3.61 \times 10^{-2}$	$4.62 \times 10^{-9} \pm 2.99 \times 10^{-9}$	$1.07 \times 10^{-4} \pm 6.95 \times 10^{-5}$

3.3. Mechanical Stability and Property

The mechanical stability and wear resistance of the superhydrophobic coating is significant in view of its usage in long-term applications. This work first used a simple method to quantify the wear resistance of the coating. The superhydrophobic surface was dragged against a 5000 grit sand paper with a 7.75 kPa normal pressure. The specimen, with exerted pressure, was moved in 40 cm cycles, rotating the specimen by 90° at the halfway point of each cycle to manifest even abrasions on the surface. After a total abrasion length of 800 cm was reached, the contact angle was measured as 138°, which indicated that the contact angle of the surface decreased as the distances of abrasion increased due to the disruption of the surface morphology. However, the surface maintained its hydrophobicity fairly well in the given distance range, as shown in Figure 7, due to the persistent nanostructures with covalently attached silane coating. The mechanical stability of the superhydrophobic surface was also characterized through ultrasonication testing in water and in a 3.5 wt % NaCl solution for 5 min. After ultrasonication in water or the 3.5 wt % NaCl solution, the surface retained its high contact angles and its superhydrophobicity as Figure 8 shows. The reduction in contact angle in case of using the NaCl solution is more than that in case of using water because of the effect of corrosive behavior of saline medium during ultrasonication. Furthermore, the influence of the 3.5 wt % NaCl solution on the mechanical property of superhydrophobic surfaces was characterized by AFM. Table 2 shows AFM images for the superhydrophobic surface, the surface after corrosion testing (after immersion in the 3.5 wt % NaCl solution for one hour), and the surface after immersion in the 3.5 wt % NaCl solution for 24 h. From three-dimensional images and roughness values (Table 2), it can be observed that the nanoscale structures on the surfaces fairly retained their sharp profile. The process of induced corrosion did not affect surface stiffness values. In other words, the surface remained firm under varying conditions. These results indicate that the superhydrophobic surface possesses favorable mechanical stability and property.

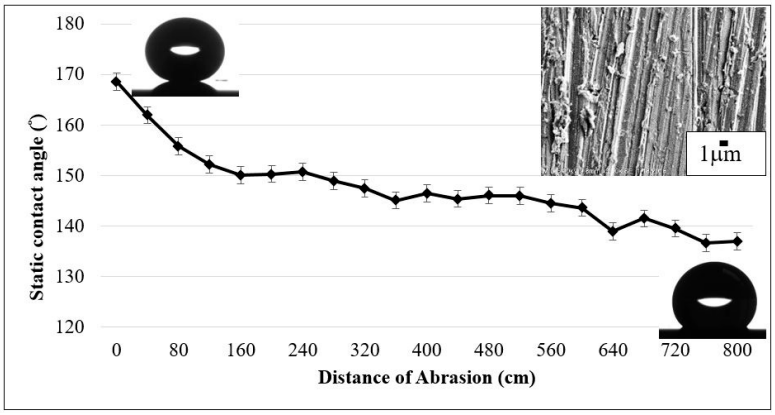

Figure 7. Water contact angles as a result of the abrasion against a 5000 grit sand paper with 7.75 kPa normal load. The inset SEM image (upper right) shows surface morphology after reaching 800 cm of abrasion length.

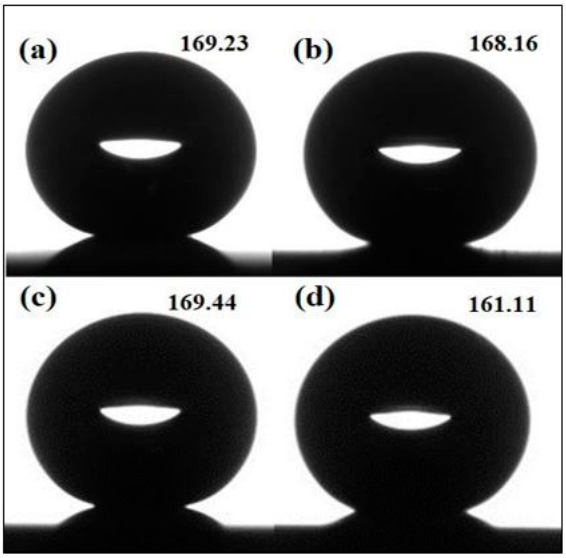

Figure 8. Static contact angle: (**a**) before ultrasonication and (**b**) after ultrasonication in water; Static contact angle (**c**) before ultrasonication and (**d**) after ultrasonication in 3.5 wt % NaCl solution.

Table 2. AFM image, roughness, and stiffness of the superhydrophobic copper surfaces.

Property	Surface		
	Superhydrophobic Copper Surface	**Superhydrophoic Copper Surface after Corrosion Test**	**Superhydrophobic Copper Surface after Immersion in 3.5 wt % NaCl for 24 h**
3-Dimensional image	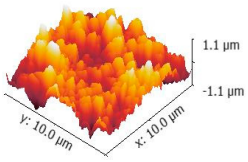	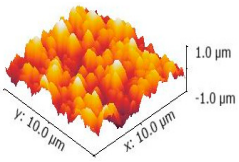	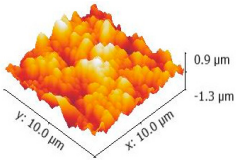
Roughness R_q (nm)	333.86 ± 5	322.54 ± 16	326.82 ± 5
Stiffness value (N/m)	4.25 ± 0.05	4.24 ± 0.26	4.23 ± 0.20

4. Conclusions

In this work, a stable and durable superhydrophobic copper surface was prepared and investigated. The superhydrophobicity of the surface was the result of the unique nanostructures on microstructures and the assembly of low surface energy components, generating a typical contact angle was around 169°. Short term immersion measurements and potentiodynamic polarization measurements revealed that the superhydrophobic copper surface exhibited an excellent corrosion resistance for the Cu substrate. Specifically, the surface retained its morphologies and surface stiffness after immersion in the 3.5 wt % NaCl solution as revealed by AFM characterization; proven to be a highly lasting treatment method. Due to its corrosion resistance and highly durable features, the superhydrophobic surface demonstrated in the current study may be presented as an effective solution for protecting copper substrates in various engineering applications.

Acknowledgments: This work was supported by Research Enhancement Grants, Lamar University. This work was also supported by grants from Center for Advances in Port Management (CAPM) of Lamar University and Center for Advances in Water and Air Quality (CAWAQ) of Lamar University to Chun-Wei Yao and Ian Lian. Özge Günaydın-Şen and Krishna Kharel were supported by Welch Foundation (V-0004).

Author Contributions: Chun-Wei Yao designed and supervised the study; Divine Sebastian, Robbie Clarke, Kirby Clayton, Chiou-Yun Chen, and Krishna Kharel performed the experiments; Divine Sebastian,

Krishna Kharel, Özge Günaydın-Şen, and Chun-Wei Yao analyzed the data; Ian Lian, Yanyu Chen and Qibo Li contributed to the research guidance; Divine Sebastian and Chun-Wei Yao wrote the paper.

Conflicts of Interest: The authors declare no conflict of interest.

References

1. She, Z.; Li, Q.; Wang, Z.; Li, L.; Chen, F.; Zhou, J. Novel method for controllable fabrication of a superhydrophobic CuO surface on AZ91D magnesium alloy. *ACS Appl. Mater. Interface* **2012**, *4*, 4348–4356. [CrossRef] [PubMed]
2. Zhu, X.; Zhang, Z.; Xu, X.; Men, X.; Yang, J.; Zhou, X.; Xue, Q. Facile fabrication of a superamphiphobic surface on the copper substrate. *J. Colloid Interface Sci.* **2012**, *367*, 443–449. [CrossRef] [PubMed]
3. Chen, Z.; Hao, L.; Chen, A.; Song, Q.; Chen, C. A rapid one-step process for fabrication of superhydrophobic surface by electrodeposition method. *Electrochim. Acta* **2012**, *59*, 168–171. [CrossRef]
4. Yao, C.-W.; Alvarado, J.L.; Marsh, C.P.; Jones, B.G.; Collins, M.K. Wetting behavior on hybrid surfaces with hydrophobic and hydrophilic properties. *Appl. Surf. Sci.* **2014**, *290*, 59–65. [CrossRef]
5. Qian, B.; Shen, Z. Fabrication of superhydrophobic surfaces by dislocation-selective chemical etching on aluminum, copper, and zinc substrates. *Langmuir* **2005**, *21*, 9007–9009. [CrossRef] [PubMed]
6. Yu, J.; Qin, L.; Hao, Y.; Kuang, S.; Bai, X.; Chong, Y.-M.; Zhang, W.; Wang, E. Vertically aligned boron nitride nanosheets: Chemical vapor synthesis, ultraviolet light emission, and superhydrophobicity. *ACS Nano* **2010**, *4*, 414–422. [CrossRef] [PubMed]
7. Chaudhary, A.; Barshilia, H.C. Nanometric multiscale rough CuO/$Cu(OH)_2$ superhydrophobic surfaces prepared by a facile one-step solution-immersion process: Transition to superhydrophilicity with oxygen plasma treatment. *J. Phys. Chem. C* **2011**, *115*, 18213–18220. [CrossRef]
8. Rao, A.V.; Latthe, S.S.; Mahadik, S.A.; Kappenstein, C. Mechanically stable and corrosion resistant superhydrophobic sol–gel coatings on copper substrate. *Appl. Surf. Sci.* **2011**, *257*, 5772–5776. [CrossRef]
9. Dong, C.; Gu, Y.; Zhong, M.; Li, L.; Sezer, K.; Ma, M.; Liu, W. Fabrication of superhydrophobic Cu surfaces with tunable regular micro and random nano-scale structures by hybrid laser texture and chemical etching. *J. Mater. Proc. Technol.* **2011**, *211*, 1234–1240. [CrossRef]
10. Wang, Z.; Li, Q.; She, Z.; Chen, F.; Li, L. Low-cost and large-scale fabrication method for an environmentally-friendly superhydrophobic coating on magnesium alloy. *J. Mater. Chem.* **2012**, *22*, 4097–4105. [CrossRef]
11. Jung, S.; Dorrestijn, M.; Raps, D.; Das, A.; Megaridis, C.M.; Poulikakos, D. Are superhydrophobic surfaces best for icephobicity? *Langmuir* **2011**, *27*, 3059–3066. [CrossRef] [PubMed]
12. Oh, J.; Birbarah, P.; Foulkes, T.; Yin, S.L.; Rentauskas, M.; Neely, J.; Pilawa-Podgurski, R.C.N.; Miljkovic, N. Jumping-droplet electronics hot-spot cooling. *Appl. Phys. Lett.* **2017**, *110*, 123107. [CrossRef]
13. Wiedenheft, K.F.; Guo, H.A.; Qu, X.; Boreyko, J.B.; Liu, F.; Zhang, K.; Eid, F.; Choudhury, A.; Li, Z.; Chen, C.-H. Hotspot cooling with jumping-drop vapor chambers. *Appl. Phys. Lett.* **2017**, *110*, 141601. [CrossRef]
14. Miljkovic, N.; Enright, R.; Nam, Y.; Lopez, K.; Dou, N.; Sack, J.; Wang, E.N. Jumping-droplet-enhanced condensation on scalable superhydrophobic nanostructured surfaces. *Nano Lett.* **2013**, *13*, 179–187. [CrossRef] [PubMed]
15. Liu, T.; Chen, S.; Cheng, S.; Tian, J.; Chang, X.; Yin, Y. Corrosion behavior of super-hydrophobic surface on copper in seawater. *Electrochim. Acta* **2007**, *52*, 8003–8007. [CrossRef]
16. Huang, Y.; Sarkar, D.K.; Gallant, D.; Chen, X.-G. Corrosion resistance properties of superhydrophobic copper surfaces fabricated by one-step electrochemical modification process. *Appl. Surf. Sci.* **2013**, *282*, 689–694. [CrossRef]
17. Wang, P.; Zhang, D.; Qiu, R.; Wan, Y.; Wu, J. Green approach to fabrication of a super-hydrophobic film on copper and the consequent corrosion resistance. *Corros. Sci.* **2014**, *80*, 366–373. [CrossRef]
18. Liu, Y.; Li, S.; Zhang, J.; Liu, J.; Han, Z.; Ren, L. Corrosion inhibition of biomimetic super-hydrophobic electrodeposition coating on copper substrate. *Corros. Sci.* **2015**, *94*, 190–196. [CrossRef]
19. Enright, R.; Miljkovic, N.; Dou, N.; Nam, Y.; Wang, E.N. Condensation on superhydrophobic copper oxide nanostructures. *J. Heat Transf.* **2013**, *135*, 091304. [CrossRef]
20. Nam, Y.; Ju, Y.S. A comparative study of the morphology and wetting characteristics of micro/nanostructured Cu surfaces for phase change heat transfer applications. *J. Adhes. Sci. Technol.* **2013**, *27*, 2163–2176. [CrossRef]

21. Chavan, S.; Cha, H.; Orejon, D.; Nawaz, K.; Singla, N.; Yeung, Y.F.; Park, D.; Kang, D.H.; Chang, Y.; Takata, Y.; et al. Heat transfer through a condensate droplet on hydrophobic and nanostructured superhydrophobic surfaces. *Langmuir* **2016**, *32*, 7774–7787. [CrossRef] [PubMed]
22. Fadeev, A.Y.; McCarthy, T.J. Self-Assembly is not the only reaction possible between alkyltrichlorosilanes and surfaces: Monomolecular and oligomeric covalently attached layers of dichloro- and trichloroalkylsilanes on silicon. *Langmuir* **2000**, *16*, 7268–7274. [CrossRef]
23. Chen, H.-H.; Anbarasan, R.; Kuo, L.-S.; Hsu, C.-C.; Chen, P.-H.; Chiang, K.-F. Fabrication of hierarchical structured superhydrophobic copper surface by in-situ method with micro/nano scaled particles. *Mater. Lett.* **2012**, *66*, 299–301. [CrossRef]
24. Yang, H.; Pi, P.; Cai, Z.-Q.; Wen, X.; Wang, X.; Cheng, J.; Yang, Z.-R. Facile preparation of super-hydrophobic and super-oleophilic silica film on stainless steel mesh via sol–gel process. *Appl. Surf. Sci.* **2010**, *256*, 4095–4102. [CrossRef]
25. Xu, W.; Liu, H.; Lu, S.; Xi, J.; Wang, Y. Fabrication of superhydrophobic surfaces with hierarchical structure through a solution-immersion process on copper and galvanized iron substrates. *Langmuir* **2008**, *24*, 10895–10900. [CrossRef] [PubMed]
26. Fransolet, A.M.; Tarte, P. Infrared spectra of analyzed samples of the amblygonite-montrebasite series: A new rapid semi-quantitative determination of fluorine. *Am. Mineral.* **1977**, *62*, 559–564.
27. Salh, R. Defect related luminescence in silicon dioxide network: A review. In *Crystalline Silicon-Properties and Uses*; Basu, S., Ed.; InTech: Rijeka, Croatia, 2011.
28. Radev, L.; Mostafa, N.Y.; Michailova, I.; Salvado, I.M.M.; Fernandes, M.H.V. In vitro bioactivity of collagen/calcium phosphate silicate composites, cross-linked with chondroitin sulfate. *Int. J. Mater. Chem.* **2012**, *2*, 1–9. [CrossRef]
29. Nimittrakoolchai, O.U.; Supothina, S. Preparation of stable ultrahydrophobic and superoleophobic silica-based coating. *J. Nanosci. Nanotechnol.* **2012**, *12*, 4962–4968. [CrossRef] [PubMed]
30. Saleema, N.; Sarkar, D.K.; Gallant, D.; Paynter, R.W.; Chen, X.G. Chemical nature of superhydrophobic aluminum alloy surfaces produced via a one-step process using fluoroalkyl-silane in a base medium. *ACS Appl. Mater. Interface* **2011**, *3*, 4775–4781. [CrossRef] [PubMed]
31. Chen, H.-H.; Anbarasan, R.; Kuo, L.-S.; Tsai, M.-Y.; Chen, P.-H.; Chiang, K.-F. Synthesis, characterizations and hydrophobicity of micro/nano scaled heptadecafluorononanoic acid decorated copper nanoparticle. *Nano Micro Lett.* **2010**, *2*, 101–105. [CrossRef]
32. Gomez-Vidal, J.C.; Morton, E. Castable cements to prevent corrosion of metals in molten salts. *Sol. Energy Mater. Sol. Cells* **2016**, *153*, 44–51. [CrossRef]
33. Su, F.; Yao, K. Facile fabrication of superhydrophobic surface with excellent mechanical abrasion and corrosion resistance on copper substrate by a novel method. *ACS Appl. Mater. Interface* **2014**, *6*, 8762–8770. [CrossRef] [PubMed]

© 2018 by the authors. Licensee MDPI, Basel, Switzerland. This article is an open access article distributed under the terms and conditions of the Creative Commons Attribution (CC BY) license (http://creativecommons.org/licenses/by/4.0/).